

## COMBINED EFFECT OF DIFFERENT FIELDS ON THE MOTION CHARACTERISTICS OF DUST PARTICLES AROUND THE INSULATORS

Jing Wang, Xi-dong Liang, Lin-hua Chen, Yu Liu  
State Key Lab of Power System, Dept. of Electrical Engineering, Tsinghua University,  
Beijing, China

\*Email: <j-w08@mails.tsinghua.edu.cn>

**Abstract:** Pollution flashover of the insulators threatens the safety and operation security of the power system severely. Contamination accumulation on the insulators is the precondition of the pollution flashover, while the contamination accumulation characteristics of the insulators depend on the motion characteristics of the dust particles moving around the insulators in service to a great degree. This paper researched the combined effect of the electric field, the air fluid field and the gravitational field on the dust particles' motion by means of experiments and numerical calculation. The distribution of the electric field and the electric potential around an actual insulator were calculated. The results indicate that the polarization force is very weak. Once the particles are charged, the electric field force acts and can drive the particles to move along the electric field lines. When there is a strong wind, the steady-state drag force is dominant and the particles move with the wind. These results can better explain the contamination accumulation characteristics of the insulators, and some measures are suggested to reduce the contamination accumulation.

### 1 INTRODUCTION

Pollution flashover of the insulators is one of the most serious accidents of the power system. The development of the insulators' pollution flashover contains the following four processes, contamination depositing, wetting of the surface, developing of the arcs, and flashover finally. So contamination accumulation is the precondition of the pollution flashover. Studying the contamination accumulation characteristics of different insulators and their influencing factors and taking measures to reduce the contamination accumulation are the effective approaches to reduce the probability of the pollution flashover.

Much work has been done and reported about the contamination accumulation characteristics of different insulators under different operating conditions [1-4]. The equivalent salt deposit density (ESDD) and non-soluble deposit density (NSDD) of the insulators were measured after a period of time exposing to the contamination. These studies indicate the following results.

- (1) The ESDD and NSDD of the upper surfaces are almost the same for different insulators, while the main difference exists on the lower surfaces of the insulators.
- (2) The on-line insulators tend to accumulate contamination more easily than the un-energized ones.
- (3) The contamination accumulation of the lower surfaces is much severer for dc insulators than ac insulators.
- (4) There is little difference of the contamination accumulation between positive and negative dc insulators.

(5) The highest ESDD and NSDD appear at the bottom of the insulator strings that connects to the high-voltage transmission line.

(6) The configurations of the insulators and the string types influence the contamination accumulation observably.

In the 1970s and 1980, many people have researched the motion characteristics of the dust particles around the insulators, on the basis of various forces acting on them. They found that the contamination accumulation characteristics were determined by the particles' motion characteristics to a great degree. However, restricted to the computing capacity, their calculation models were oversimplified [5-10].

In this paper, the main four forces, which are the polarization force, the electric field force, the steady-state drag force and the gravitational force, were analyzed. Their effects on the particles' motion were studied by both experiments and numerical calculation.

The effect of electric field was studied by the coaxial electrode model experiments. A simplified 2D axial symmetric calculation model was built to simulate the particles' moving trajectories under the combined effect of these forces. The simulation resulted in good coincidence with the experimental phenomenon. In the end, the distribution of the electric field and the electric potential around a 1000 kV dc insulator were calculated. On the basis of the influence of the forces on the dust particles' motion, the contamination accumulation characteristics of different insulators can be better explained.

## 2 FORCE ANALYSIS

In order to research the motion characteristics of the dust particles, the forces acting on them have to be analyzed. Many forces act on the particles around the on-line insulators due to the effects of the combined fields. The main four forces are analyzed as follows. The theoretical prediction is based on the assumption that all particles are spherical.

### 2.1 Polarization force

Since the permittivity of the dust particles is larger than that of the air generally, for particles in the electric field, they will be polarized and polarization charge will be generated at the two ends of the particles. Then the polarization force will act on them. For any particles in non-uniform electric field, charged or uncharged, this force always acts. The polarization force can be expressed by (1).

$$\vec{F}_p = 2\pi a^3 \varepsilon_0 \times \frac{\varepsilon_r - 1}{\varepsilon_r + 2} \times \text{grad} \vec{E}^2 \quad (1)$$

Where:  $a$  = radius of the particle in meter (m)  
 $\varepsilon_0$  = vacuum permittivity in Ferrari per meter (F/m)  
 $\varepsilon_r$  = relative permittivity of the particles (dimensionless)  
 $E$  = strength of electric field in volt per meter (V/m)

The direction of  $\vec{F}_p$  is the same as  $\text{grad} \vec{E}^2$ , which points to the direction in which the strength of electric field increases. When the electric field is uniform, this force equals zero.

### 2.2 Electric field force

Most of the dust particles in the air are charged. There are three mechanisms by which aerosol particles acquire charge, static electrification, diffusion charging and field charging. If corona discharge produces unipolar ions in the space, field charging is the dominant mechanism for particles larger than 1.0  $\mu\text{m}$ , and the saturation charge for the particle is:

$$q_{ps} = \frac{12\varepsilon_r}{\varepsilon_r + 2} \pi \varepsilon_0 a^2 E_0 \quad (2)$$

Where:  $E_0$  = corona onset strength of electric field in volt per meter (V/m)

The electric field force is expressed by (3). The electric field force acting on the charged particles was zero due to the alternation nature of the ac voltage.

$$\vec{F}_e = q\vec{E} \quad (3)$$

Where:  $q$  = quantity of charge carried by the particle in Coulomb (C)

### 2.3 Steady-state drag force

The particles interact with the air when they are moving in the air fluid. Many kinds of forces will be induced by the particle-fluid interaction, in which the steady-state drag force is the most important one, while the other forces are very small and can be ignored. The "steady-state" means that there is no acceleration of the relative velocity between the particle and the air fluid. Since the air flow carrying the particles is in the Stokes flow regime, the drag force can be expressed by (4).

$$\vec{F}_D = 6\pi\mu a(\vec{u} - \vec{v}) \quad (4)$$

Where:  $\mu$  = kinetic viscosity of the air in Pascal multiplied by second (Pa · s)

$\vec{u}$  = velocity of the air in meter per second (m/s)

$\vec{v}$  = velocity of the particle in meter per second (m/s)

### 2.4 Gravitational force

The gravitational force acting on the particle is expressed by (5).

$$\vec{G} = \frac{4}{3}\pi a^3 \rho_p \vec{g} \quad (5)$$

Where:  $\rho_p$  = density of the particle in gram (g)

$\vec{g}$  = acceleration of gravity in meter per square second (m/s<sup>2</sup>)

According to Newton's Second Law, the equation of motion for a particle can be expressed as (6).

$$m \frac{d\vec{v}}{dt} = \vec{F}_p + \vec{F}_e + \vec{F}_D + \vec{G} \quad (6)$$

Integrating the particle's velocity  $\vec{v}$  on the time intervals, the particle's moving trajectory can be calculated.

## 3 EXPERIMENTS

A coaxial electrode was designed to study the effect of the electric field on the particles' trajectories. The schematic diagram of the experimental device is illustrated in Figure1. It contained a grounded aluminous tube with length  $L = 0.5$  m, and radius  $R = 0.25$  m, in which a stainless-steel cylinder with radius  $r = 0.002$  m was located along the axis. The inner electrode was connected to the dc or ac voltage source. Particles enclosed in a small fixed cylinder were scattered by a shaking griddle and dropped to the

space between the electrodes. The tested particles used in this research were the talcum powder, with volume weighted mean diameter  $D = 22.86 \mu\text{m}$ , relative permittivity  $\epsilon_r = 11$ , and density  $\rho = 2700 \text{ kg/m}^3$ . The following experiment and calculation results were based on this kind of talcum powder.

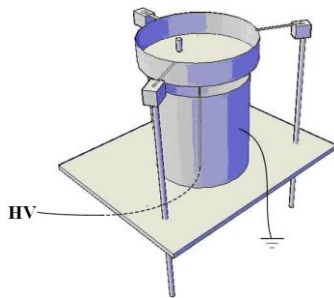


Figure 1: Schematic diagram of the experimental device

### 3.1 Below the corona onset voltage

Lower electric potential  $V = 20 \text{ kV ac}$  was applied to the inner electrode. Such low voltage couldn't induce the corona. Just the polarization force acted on the particles due to the ac electric field. When the particles were released over a distance from the inner electrode, they dropped vertically without deflection. However, when the particles were released near the inner electrode, they deflected and part of them adhered to the inner electrode as shown in Figure 2.

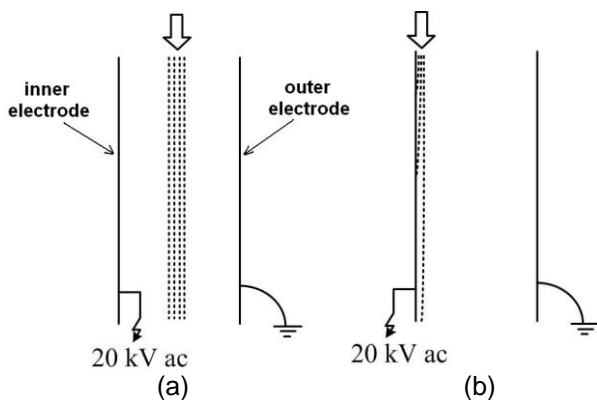


Fig 2: Particles' trajectories in the ac electric field without corona: (a) released over a distance from the inner electrode; (b) released near the inner electrode

### 3.2 Above the corona onset voltage

Higher electric potential  $V = \pm 55 \text{ kV dc}$  was applied to the inner electrode, and it was high enough to sustain a corona regime in the stationary state. The ions, with the same polarity as the voltage, travelled toward the outer electrode, collided with the particles and charged the particles. This was the process of field charging of the talcum powder particles. The particles were repelled by the inner electrode, drifted and most of them adhered to the outer electrode as shown in Figure 3 (a). The experimental phenomena were

almost the same under the positive and negative dc voltage.

Then electric potential  $V = 40 \text{ kV ac}$  was applied and an unstable corona was produced. The particles' trajectories are shown in Figure 3(b). Because the polarity of the inner electrode and the space ions changed continually, the polarity of the charged particles and the direction of the electric field force changed consequently. This process was very complicated, and resulted in the wavy trajectories of the particles. But few particles adhered to the electrodes.

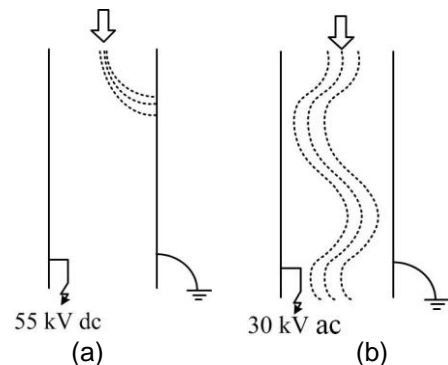


Figure 3: Particles' trajectories in the dc and ac electric field with corona: (a) 55 kV dc corona (b) 40 kV ac corona

## 4 CALCULATION

The experimental coaxial electrode was simplified to a 2D axial symmetric calculation model. The electric potential of the inner electrode and the top shielding ball was set to a certain value according to the experiments and the other sides of the model were all grounded. The upper side and nether side were set as the wind inlet and outlet boundaries separately. The parameters of the particles were set the same as the talcum powder. Use finite element method to calculate the model.

### 4.1 Effect of the polarization force

The electric potential was set to 20 kV. The particles' trajectories were calculated under the influence of the polarization force, the gravitational force and the steady-state drag force, as shown in Figure 4 (a). The radial polarization force acting on the particles along the radius of the coaxial electrode is shown in Figure 5. It demonstrates that the strength of electric field decreases drastically near the inner electrode and most part of the electric field is quasi-uniform. As a result, the polarization force is stronger in close proximity to the inner electrode and approximate zero over a certain distance from the inner electrode.

### 4.2 Effect of the electric field force

The electric potential was set to 55 kV and the particles were supposed to be saturated charged. Their trajectories were calculated under the

combined influence of the electric field force, the polarization force, the gravitational force and the steady-state drag force, as shown in Figure 4 (b).

The strength of radial electric field was calculated as shown in Figure 6. Because the precision of the mesh was finite, a tip angle was present on the curve where its curvature changed dramatically, but this didn't influence the trend of the whole curve. The radial electric field force, the radial polarization force and the gravitational force acting on the charged particles were calculated along the radius, as shown in Figure 7. The steady-state drag force was time-variable with the change of the particle's velocity, so it wasn't calculated to compare with the other three forces.

It can be seen that the electric field force is much larger than the gravitational force where the electric field strength is high and it's comparable with the gravitational force where the electric field strength is low. The polarization force is much smaller than the other forces, so its effect can be ignored. These results indicate that the electric field force is the dominant force for charged particles moving in the still air with the presence of a strong electric field.

### 4.3 Effect of the fluid drag force

The wind fields were calculated when the inlet wind velocities were set to 0.1 m/s, 1 m/s and 3 m/s successively, which represented calm, light air and light breeze separately. The electric potential of the inner electrode was kept at 55 kV. Supposing the particles were saturated charged, the particles' trajectories under the combined effect of the four forces were calculated as shown in Figure 8. It can be deduced that when the wind is strong, the steady-state drag force is dominant and the particles move with the wind.

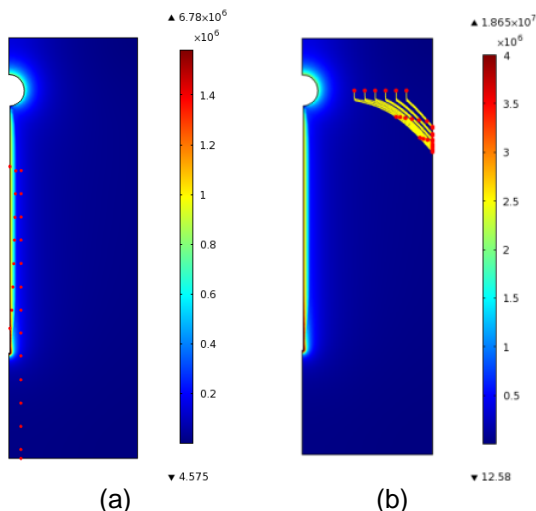


Figure 4: Calculated trajectories of the particles (strength of the electric field as surface map, V/m): (a) Effect of the polarization force on the neutral particles' motion (b) Effect of the electric field force on the charged particles' motion

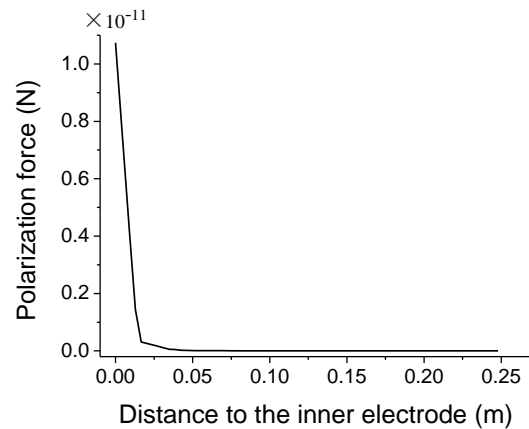


Figure 5: Polarization force acting on the neutral particles along the radius of the coaxial electrode

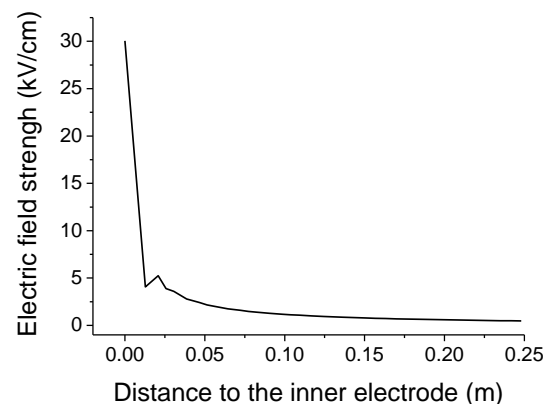


Figure 6: The strength of the electric field along the radius of the coaxial electrode

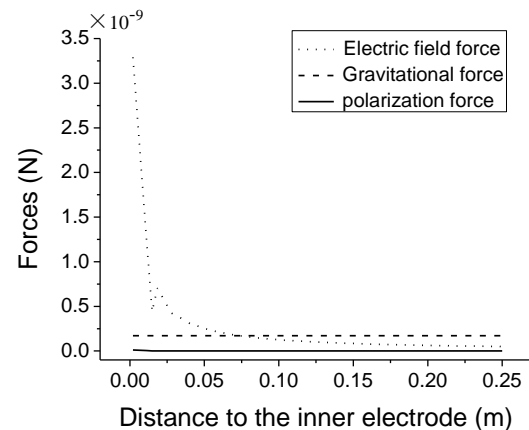


Figure 7: Forces acting on the charged particles along the radius of the coaxial electrode

### 4.4 Electric field around the insulator

According to the above results, it can be seen that the dc electric field force acting on the charged particles is remarkable. A full-size 3D calculation model of the 1000 kV dc composite insulator hanging on the cross arm of the tower and suspending the transmission line was built, as shown in Figure 9. The length of the insulator was about 11 m. Use charge simulation method and boundary element method to calculate the electric

field and potential distribution around the insulator. The results are shown in Figure 10.

The equal potential lines are almost perpendicular to the axis of the insulator. So the electric field between the neighbouring sheds is parallel to the axis. When the low-speed charged dust particles come to the neighbourhood of the sheds, they will deflect along the electric field line and deposit on the surface. The strength of the electric field along the sheath of the insulator is shown in Figure 11. The electric field strength is highest at the high-voltage terminal, low in the middle part, and increases at the grounded terminal, presenting a “U” curve. The actual contamination distribution of the insulator presents the similar trend [11].

## 5 DISCUSSION

The electric field force is the main reason causing the different contamination accumulation characteristics between the dc and ac insulators. Most of the dust particles in the air are charged through various ways. The conductive particles can capture more ions than the insulating ones, so

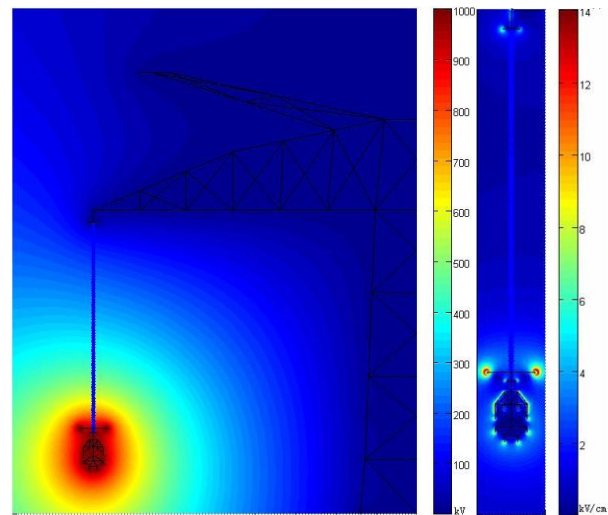


Figure 10: (a) Electric potential distribution around the insulator (b) Electric field distribution around the insulator

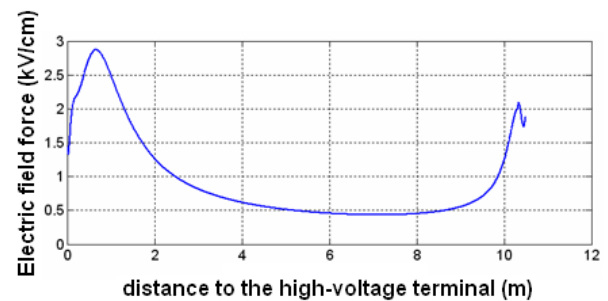


Figure 11: Strength of electric field along the sheath of the insulator

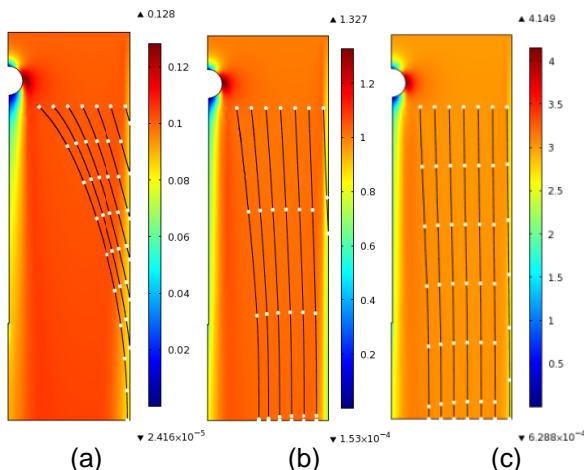


Figure 8: Calculated trajectories of the charged particles when both corona and wind exist (wind velocity field as surface map, m/s) (a)  $V_{inlet} = 0.1$  m/s; (b)  $V_{inlet} = 1$  m/s; (c)  $V_{inlet} = 3$  m/s

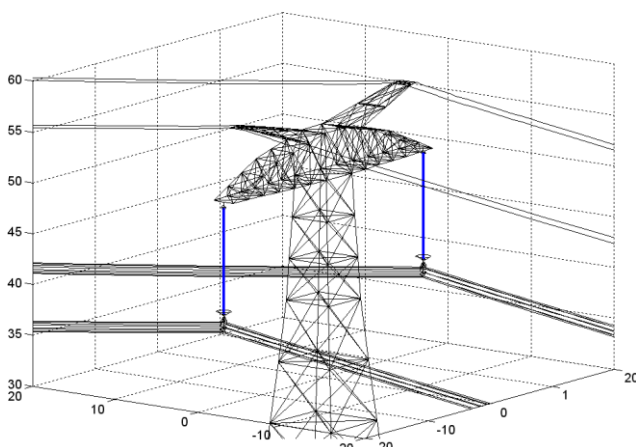


Figure 9: Full-size 3D calculation model for the 1000 kV dc insulator

more conductive particles are adhered to the dc insulators, resulting in the different constituents of the contamination layer between dc and ac insulators. In order to decrease the number of charged particles, the voltage-sharing measures should be adopted to reduce the corona of the high-voltage terminal.

For a saturated charged particle, the electric field force is proportional to the square of its radius, while the gravitational force is proportional to the cube of its radius. So the smaller charged particles can adhere to the lower surface more easily under the influence of the electric field force, while the bigger particles tend to drop on the upper surface. So the average diameter of the particles on the lower surface is smaller than the upper surface. Controlling the electric field around the insulator to a lower level can reduce the contamination accumulation of the dc insulators.

The fluid characteristics around the insulators are determined by their configurations. If there are deep ribs under the sheds, the wind will be obstructed and form vortices [12]. The velocity of the wind and the carried particles will drop sharply, providing chance for the particles to deposit under the electric field force. Rational design of the configuration aiming to prevent the formation of

vortexes is an effective way to reduce the contamination accumulation of all insulators.

## 6 CONCLUSION

- (1) The dust particles are moving under the combined effect of the electric field, the air fluid field and the gravitational field around the insulators. The contamination accumulation characteristics of the insulators are determined by the motion characteristics of the dust particles to a great degree.
- (2) Attraction of the uncharged particles by the polarization force can be neglected since there is no necessary strong change of the electric field around the insulators.
- (3) The direction of the ac electric field force acting on the charged particles alternates rapidly, so the total effect is very weak in contrast with the dc electric field force. This is why the contamination accumulation of the lower surfaces is much severer for dc insulators than ac insulators.
- (4) When the wind is strong, the steady-state drag force is dominant. Aerodynamic shed configuration which can reduce the formation of the vortexes should be chosen for porcelain insulators in the highly-polluted areas.

## 7 ACKNOWLEDGMENTS

This work has been supported financially by the Foundation of State Key Laboratory of Tsinghua University and the Major State Basic Research Development Program of China (973 Program).

## 8 REFERENCES

- [1] Wang Bin, Liang Xi-dong, Zhang Yi-bo et al: "Natural Pollution Test of Composite and Porcelain Insulators Under AC and DC stress", *High Voltage Engineering*, Vol. 35, No. 9, pp. 2322-2328, 2009
- [2] Gao Hai-feng, Fan Ling-meng, Li Qing-feng et al: "Comparative Analysis on Pollution Deposited Performances of Insulators on the  $\pm 500$  kV Gao-Zhao DC Transmission Line", *High Voltage Engineering*, Vol. 36, No. 3, pp. 672-677, 2010
- [3] Li Zheng-yu, Liang Xi-dong, Wang Bin and Zhou Yuan-xiang: "Natural Pollution Deposit Test of Polymeric Insulators Operated under DC Voltage", *Power System Technology*, vol. 31, No. 14, pp.10-14, 2007
- [4] Su Zhi-yi, Liu Yan-sheng: "Comparison of Natural Contaminants Accumulated on Surfaces of Suspension and Post Insulators with DC and AC Stress in Northern China's

Inland areas", *Power System Technology*, Vol. 28, No. 10, pp.13-17, 2004

- [5] A.K.Gertsik, A. V. Korsuntser, N. K. Nikol'skii: "The Effect of Fouling on Insulators for HVDC Overhead Lines", *Direct Current*, pp 219-226, 1957
- [6] H. Haerer: "Insulators for High Voltage Direct Current Under Contamination Conditions", Ph.D. Thesis, University of Stuttgart, Stuttgart, Germany, 1971
- [7] R. G. Olsen, B. C. Furumasa and D. P. Hartmann: "Contamination Mechanisms for HVDC Insulators", *IEEE Power Apparatus and Systems Winter Conference*, New York, America, Paper A 77-035-9, 1977
- [8] R. G. Olsen, J. Daffe: "The Effect of Electric Field Modification and Wind on the HVDC Insulator Contamination Process", *IEEE Power Apparatus and Systems Winter Conference*, New York, America, Paper A 78-120-8, 1978
- [9] Mark N. Horenstein, James R. Melcher: "Particle Contamination of High Voltage DC Insulators Below Corona Threshold", *IEEE Transactions on Electrical Insulation*, Vol. EI-14, No. 6, pp. 297-305, 1979
- [10] V. Radun, J. R. Melcher: "DC Power Line Charging of Macroscopic Particles and Associated Electrical Precipitation on Insulators", *IEEE Transactions on Electrical Insulation*, Vol. EI-16, No. 3, pp. 165-179, 1981
- [11] Zhang Kai-xian: "Rule of Distribution of Natural Pollution Deposition on Suspension Insulator String", *Power System Technology*, Vol 21, No. 3, pp. 39-43, 1997
- [12] JIANG Xing-liang, LI Hai-bo: "Application of Computational Fluid Dynamics to Analysis of Contamination Depositing Characteristics of Insulators", *High Voltage Engineering*, Vol. 36, No. 2, pp. 329-334, 2010